Digital Computer Laboratory
Massachusetts Institute of Technology
Cambridge, Massachusetts

SUBJECT: GROUP 63 SEMINAR ON MAGNETISM, LII

To: Group 63 Staff

From: Arthur L. Loeb and Norman Menyuk

Date: May 29, 1953

The two previous reports discussed the magnetization of the ferrites at absolute zero temperature and at the Curie point. In this report the variation of the spontaneous magnetization in the region of absolute zero temperature will be considered. For this study it is convenient to consider the region FCE, in which both sub-lattices are saturated, separately from regions ACF and BCE, in which only one of the sub-lattices is saturated.

A.) Only one sub-lattice saturated

Let us consider region ACF (Figure 108) in which sub-lattice B is saturated and sub-lattice A is unsaturated.

At meeting 50, equation 2, it was found that the partial spontaneous magnetizations are

$$\vec{I}_a = MB_j\left[\frac{M\vec{h}_a}{RT}\right]$$

$$\vec{I}_b = MB_j\left[\frac{M\vec{h}_b}{RT}\right] \qquad 2$$

Furthermore, from meeting 49, equations 10 and 11, we have the relations

$$\vec{h}_a = n\,(\alpha\lambda\vec{I}_a + \mathcal{E}\mu\vec{I}_b) \qquad \text{XLIX-10}$$

$$\vec{h}_b = n\,(\beta\mu\vec{I}_b + \mathcal{E}\lambda\vec{I}_a). \qquad \text{XLIX-11}$$

Since we are considering the case of anti-parallel alignment of the A and B sites, $\mathcal{E} = -1$ and $\vec{I}_a$ is aligned anti-parallel to $\vec{I}_b$. The above equations can therefore be rewritten as algebraic equations, namely

$$h_a = n\,(\alpha\lambda I_a + \mu I_b) \qquad \text{LII-1}$$

$$h_b = n\,(\beta\mu I_b + \lambda I_a). \qquad \text{LII-2}$$

At meeting 50, we found that in region ACF at absolute zero temperature $I_b = M$ and $I_a = -\frac{\mu}{\lambda\alpha} M$. Therefore, at absolute zero

$$h_a = 0$$

$$h_b = n \mu M (\beta - \frac{1}{\alpha}) > 0$$

The Brillouin function was defined (meeting 49) as

$$B_j [Z] = \frac{2j+1}{2j} \coth \frac{(2j+1)Z}{2j} - \frac{1}{2j} \coth \frac{Z}{2j}$$

where

$$Z = \frac{Mh}{RT} \quad \text{for } H = 0.$$

For low temperatures, Z is therefore large.

Consider the function coth x where x is large

$$\text{Coth } x = \frac{e^x + e^{-x}}{e^x - e^{-x}} \approx 1 + 2e^{-2x}$$

Therefore, for Z large,

$$B_j [Z] = \frac{2j+1}{2j} \left[1 + 2e^{-\frac{2j+1}{2j} Z} \right] - \frac{1}{2j} \left[1 + 2e^{-\frac{Z}{2j}} \right]$$

$$B_j [Z] = 1 - \frac{e^{-\frac{Z}{j}}}{j} \left[1 - (2j+1) e^{-2Z} \right] \approx 1 - \frac{e^{-\frac{Z}{j}}}{j} \qquad \text{LII-3}$$

The Brillouin function appears graphically as shown in Figure 112. The curve 01A represents the Brillouin function at temperature $T = 0^\circ K$, while the curve Γ represents the Brillouin function at a low but finite temperature. The representative points of the molecular field at $T = 0^\circ K$ are denoted as h_a and h_b. It can be seen that the Brillouin function $B\left[\frac{Mh}{RT}\right]$ is unity at zero temperature. At $h = h_a = 0$, on the other hand, the Brillouin function is inderterminate, lying between zero and unity.

At the slightly higher temperature for which the Brillouin curve has shifted to Γ, the representative molecular field points will also shift slightly. These new points are represented by h_a' and h_b'. Since h_a' is in the region of sharp rise of the Brillouin function there will be a marked change in I_a with temperature. However, h_b' lies beyond the bend of the Γ curve and there is very little change in I_b with temperature. It will remain approximately equal to M, the saturation value. The value of I_b will therefore be assumed equal to M in the low temperature region, and

we shall investigate the thermal variation of I_a with temperature.

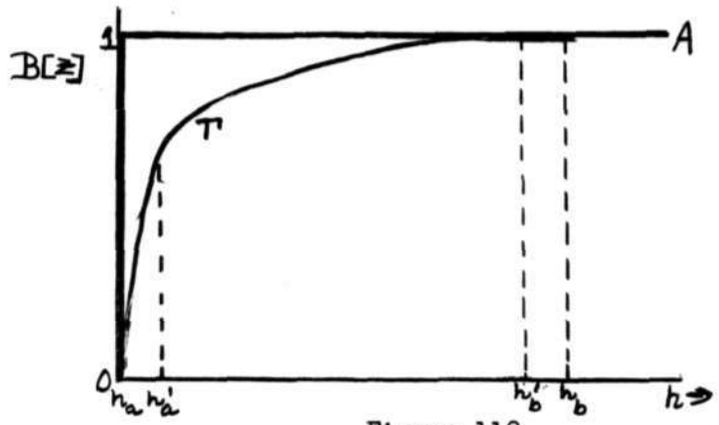

Figure 112

Assuming $I_b = M$, equation LII-1 may be rewritten as

$$I_a = \frac{h_a - \mu n M}{\alpha \lambda M} \qquad \text{LII-4}$$

Equations L-2 and LII-4 give two equations involving I_a as a function of the molecular field h_a. Equation LII-4 is independent of temperature, but in equation L-2 I_a appears as a function of temperature as well as the molecular field. The solution of I_a as a function of temperature must satisfy both equations simultaneously. In the graphical solution which follows, this solution is represented by the point of intersection of the curves of the two equations.

At absolute zero temperature, equation L-2 gives rise to the magnetization curve OMT of Figure 113. At a finite temperature near absolute zero the magnetization curve has the form given by T; at a still higher temperature the curve is as shown by T'.

Equation LII-4 is the equation of a straight line Δ which cuts the curve OMT at the point Q, where $OQ = -\frac{\mu n}{\alpha \lambda} M$ represents the magnetization of sub-lattice A at 0°K. At the temperature for which the line T' is the solution of equation L-2, the new representative point of the spontaneous magnetization of the A sites becomes Q'. Similarly, at a still higher temperature the magnetization of the A sites is given by Q''.

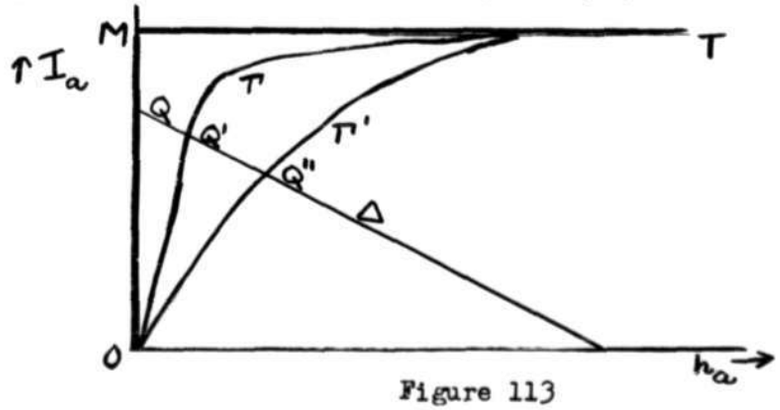

Figure 113

Thus the magnetization of the unsaturated A sites decreases much more rapidly than the saturated B sites upon increasing the temperature.

The saturation magnetization $I_s = |\lambda I_a - \mu I_b|$ and in region ACF the partial magnetization of the unsaturated sites is smaller than the partial magnetization of the saturated sites ($\lambda I_a < \mu I_b$). Therefore a decrease in the magnetization of the unsaturated sites causes an increase in the total magnetization (see Figure 114), so that in region ACF the total magnetization increases with temperature.

The above discussion is equally valid in region BSH on interchanging λI_a and μI_b.

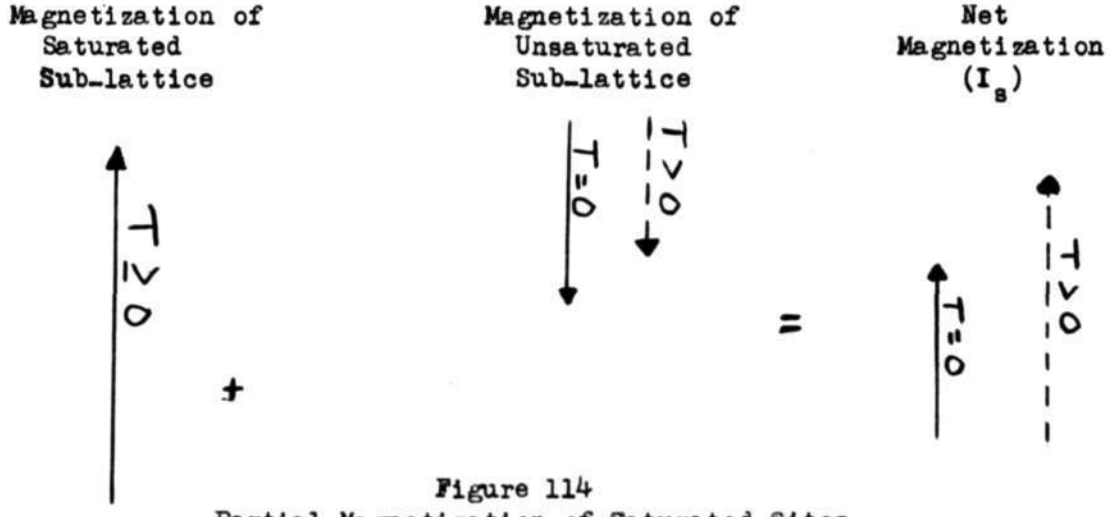

Figure 114
Partial Magnetization of Saturated Sites
Exceeds that of Unsaturated Sites

The thermal variation of the magnetization in regions ACF and BSH therefore appears as shown in Figure 115.

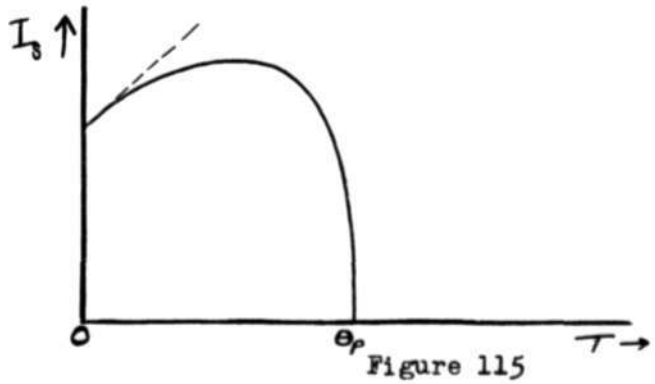

Figure 115

On the other hand, in region ECSH of Figure 108, the partial magnetization of the unsaturated sub-lattice has a greater absolute value than the partial magnetization of the saturated sub-lattice ($I_a > I_b$ but $\lambda I_a < \mu I_b$). The total magnetization will therefore decrease on increasing the temperature (see Figure 116).

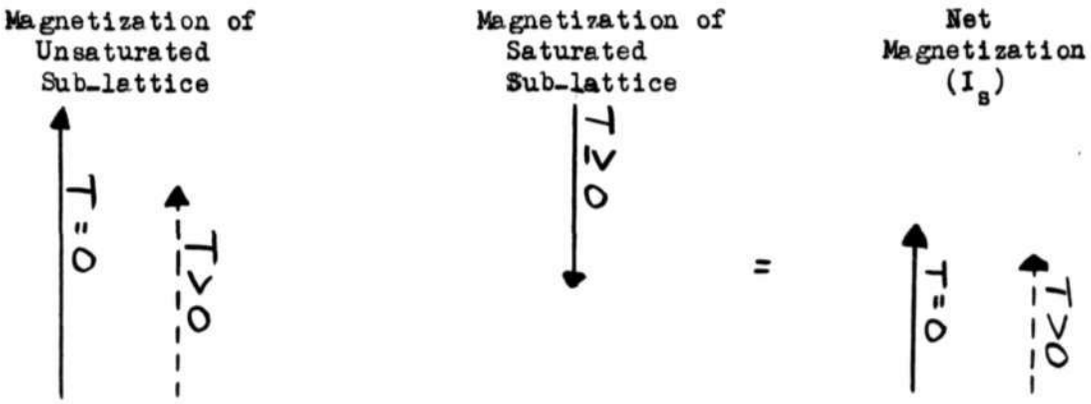

Figure 116
Partial Magnetization of Unsaturated Sites
Exceeds that of Saturated Sites

The magnetization variation with temperature will then appear as shown in Figures 117(a) and (b). Curve 117(a) is the shape of the curve for that portion of ECSH which falls within the triangular region DSH of Figure 109; the occurrence of two Curie points in region DSH was discussed at Meeting 51.

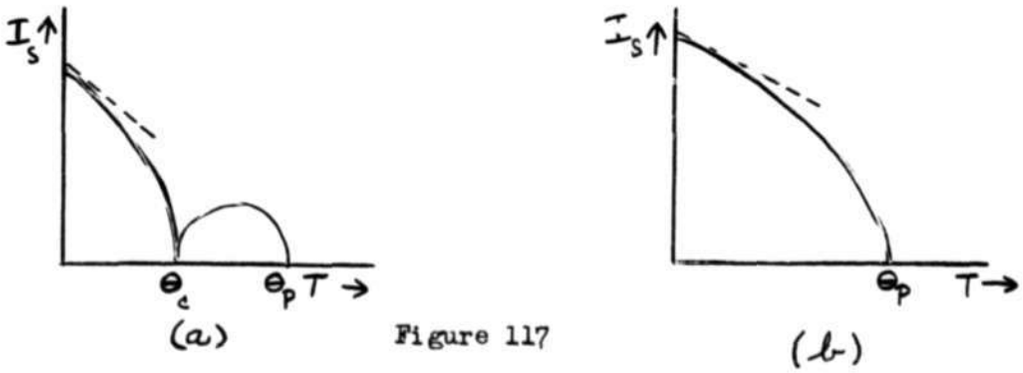

Figure 117

B.) Both sub-lattices saturated (Region FCE)

When both sub-lattices are saturated, the variation of the partial magnetization of each of these sub-lattices will be zero at the absolute zero temperature. At temperatures slightly above absolute zero, this variation will be small but finite. In order to determine the relative magnitude of this variation of the partial magnetizations in the low temperature regions, we make use of the low temperature approximation of the Brillouin function derived above; namely

$$B_j[z] = 1 - \frac{1}{j} e^{-\frac{z}{j}}$$

As discussed at meeting 50 and above,

$$\left.\begin{aligned} \vec{I}_a &= MB_j\left[\frac{\vec{Mh}_a}{RT}\right] \\ \vec{I}_b &= MBj\left[\frac{\vec{Mh}_b}{RT}\right] \end{aligned}\right\} \qquad \text{L-2}$$

and the net magnetization

$$I_s = \left|\lambda I_{as} - \mu I_{bs}\right| . \qquad \text{L-1}$$

At low temperatures the molecular fields $\vec{h}_a$ and $\vec{h}_b$ are very close to their values at absolute zero, namely:

$$\left.\begin{aligned} h_a &= Mn(\lambda\alpha + \mu) \\ h_b &= Mn(\mu\beta + \lambda). \end{aligned}\right\} \qquad \text{LII-5}$$

From the above sets of equations one finds

$$I_s = M\left[\mu - \lambda + \frac{\lambda}{j} e^{-\frac{Mn(\lambda\alpha+\mu)}{RT}} - \frac{\mu}{j} e^{-\frac{Mn(\mu\beta+\lambda)}{RT}}\right] \qquad \text{LII-6}$$

Let us examine the temperature variation of the more general function.

$$f(T) = A + B + C\, e^{-\frac{p}{T}} + De^{-\frac{q}{T}}$$

$$\frac{df(T)}{dT} = \frac{pC}{T^2} e^{-\frac{p}{T}} + \frac{qD}{T^2} e^{-\frac{q}{T}}$$

Define $p > q$

$$\frac{df(T)}{dT} = e^{-\frac{q}{T}}\left[\frac{pC}{T^2} e^{-\frac{(p-q)}{T^2}} + \frac{qD}{T^2}\right]$$

For T small and $p > q$, the exponential term is very small. Therefore

$$\frac{df(T)}{dT} = \frac{qD}{T^2} e^{-\frac{q}{T}}$$

Thus the term with the larger exponent effectively drops out, and the term with the smaller exponent is dominant. Both exponentials have the same value when

$$\lambda\alpha + \mu = \mu\beta + \lambda. \qquad \text{III-7}$$

This equation is represented by the line CK in Figure 118, passing through the point $\alpha = 1$, $\beta = 1$ and parallel to SD.

In the region FCK, $\mu\beta + \lambda > \lambda\alpha + \mu$. Therefore,

$$\frac{dI_s}{dT} = \frac{\lambda Mn(\alpha\lambda + \mu)}{jT^2} e^{-\frac{Mn(\alpha\lambda + \mu)}{T}} > 0$$

and the magnetization increases with temperature in the neighborhood of absolute zero.

Similarly, in region KCE, $\lambda\alpha + \mu > \mu\beta + \lambda$ and

$$\frac{dI_s}{dT} = -\frac{\mu Mn(\mu\beta + \lambda)}{jT^2} e^{-\frac{Mn(\mu\beta + \lambda)}{T}} < 0$$

so the magnetization decreases with increasing temperature in the low temperature region.

However, the magnetization curve is horizontal in both regions at the absolute zero temperature. The resultant magnetization curves are shown in Figure 118 (Q), (P), and (N).

Summary

The results of the last two lectures may be summarized in terms of the following diagrams. Figure 118 indicates the various regions of the $\alpha\beta$ plane while Figure 119 shows the predicted shapes of the magnetization curve for each of these regions.

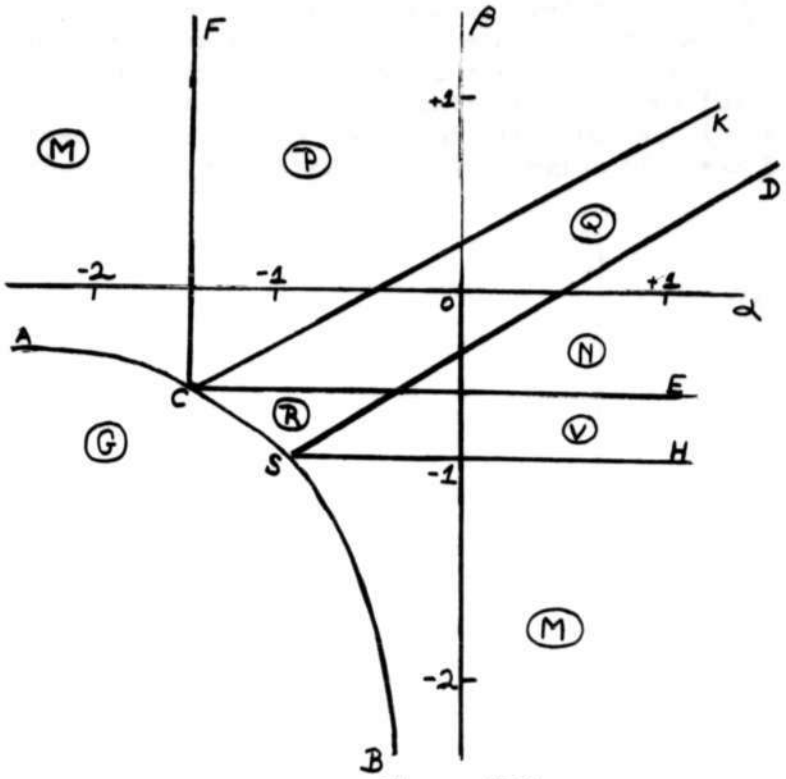

Figure 118

α-β Plane Assuming $\mathcal{E} = -1$ and $\frac{\lambda}{\mu} = \frac{2}{3}$

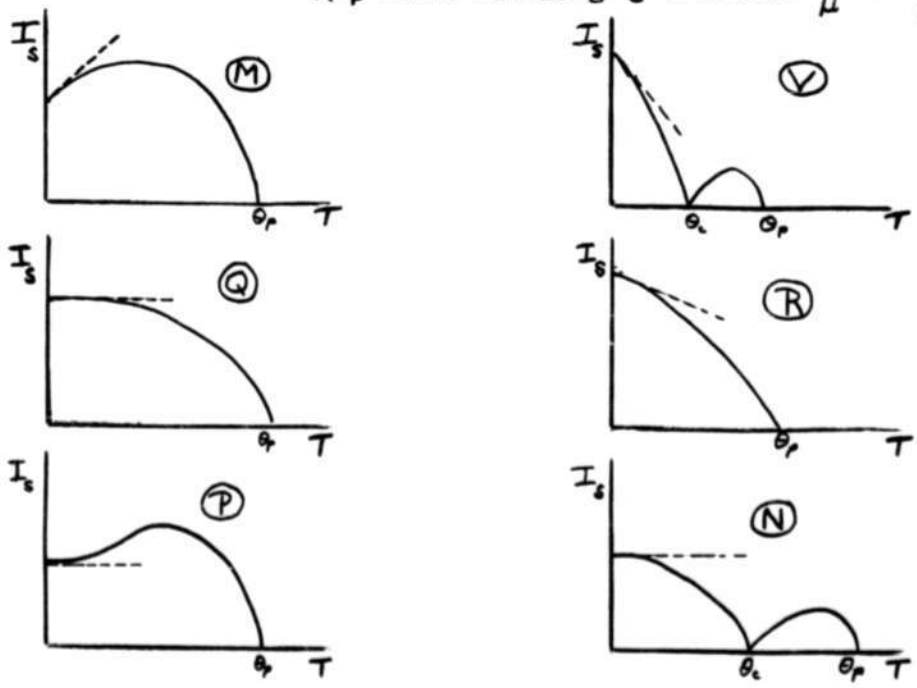

Figure 119

Possible Types of Magnetization Curves
(Circled letters indicate regions of α-β plane to which curves correspond)

Most of the magnetization curves predicted by Néel, and shown in Figure 119 had not been observed experimentally at that time (1947). However, at the 1953 Spring Meeting of the American Physical Society, L. R. Maxwell* presented various magnetization curves for different materials which exhibited the predicted characteristic shapes. These curves are shown in Figure 120 for several materials. The region of the $\alpha\beta$ plane is indicated for each case.

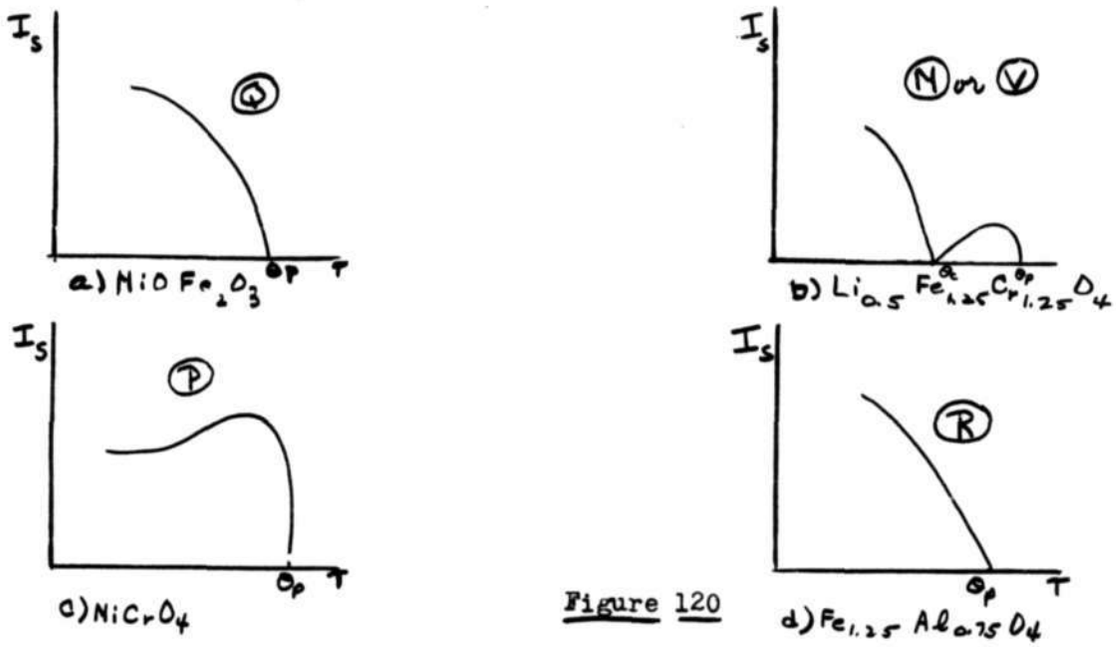

Figure 120

It is uncertain whether the magnetization curve of $Li_{0.5}Fe_{1.25}Cr_{1.25}O_4$ (Figure 120b) is of the (V) or (N) type since the temperature was not low enough to ascertain the slope of the magnetization at absolute zero. The shape of the curve as given indicates it is probably a (V) type curve.

These curves represent a strong verification of the Néel theory.

Signed _____
Arthur L. Loeb

_____
Norman Menyuk

Approved _____
David R. Brown

ALL/NM;jk
Group 62 (25)

* L. R. Maxwell, Trivalent Substitutions in the Ferrites